

# Modeling Poly(Vinyl Alcohol)-Stabilized Vinyl Acetate Emulsion Polymerization. II. Comparison With Experiment

C. M. GILMORE, G. W. POEHLEIN, and F. J. SCHORK\*

Georgia Institute of Technology, Atlanta, Georgia 30332

## SYNOPSIS

The mathematical model presented in Part I, accommodating the emulsion polymerization of vinyl acetate stabilized with poly(vinyl alcohol), predicts experimental conversion and particle size data with reasonable accuracy. Model predictions of measurable variables exhibit sensitivity to variables affecting either primary ungrafted particle nucleation or flocculation kinetics, but are relatively insensitive to variables affecting poly(vinyl alcohol) grafting reactions and the resulting primary grafted particle concentration. Semibatch simulations indicate that independent increases in the vinyl acetate, poly(vinyl alcohol), and initiator levels all increase the primary grafted particle population. It is unlikely, however, that this population exceeds the ungrafted counterpart under most commercial polymerization conditions. This relative insignificance of grafting during particle nucleation is also noted in literature data simulations where, with appropriate parameter adjustments, the model predictions agree well with the batch, thermal initiation data. © 1993 John Wiley & Sons, Inc.

## INTRODUCTION

The first of this two-part paper details a mathematical model for particle nucleation and growth in the emulsion polymerization of vinyl acetate stabilized with poly(vinyl alcohol). Here, the model is validated by simulating semibatch and batch experimental conversion and particle size/number profiles. Its utility is further demonstrated by the prediction of unmeasurable species concentrations to clarify the nucleation process.

First, a semibatch, redox initiation recipe is used to demonstrate variable selection and model sensitivity. This base recipe is augmented by model simulations to show how particle nucleation and resulting measurable parameters are influenced by recipe changes. Next, model versatility is demonstrated by the simulation of data from batch reactions that employ thermal initiators. These data span a range of experimental conditions.

## EXPERIMENTAL

### Semibatch Simulations

The base semibatch recipe, presented in Table I, is a simple vinyl acetate homopolymerization at 25% solids. (Note that the base designation earmarks this recipe as a reference for later discussion of simulation results, but does not imply any special theoretical significance to the associated base reaction parameters.)

The vinyl acetate and Vinol 205, a nominally 88% hydrolyzed, low molecular weight ( $\bar{M}_v$  11,000–31,000) poly(vinyl alcohol), were obtained from Air Products and Chemicals, Inc. The vinyl acetate was inhibited with 3–5 ppm hydroquinone, and was used as received. Calculations suggest that this low hydroquinone level would only delay the polymerization by about 5 s. The Vinol 205 solution was prepared by slowly adding 200 g of the polymer to 1800 mL of agitated 50°C deionized water. The solution was then heated to 90°C and held for 2 h with agitation to ensure solubilization of the poly(vinyl alcohol). The final solution was clear and gel-free. The hydrogen peroxide, ferrous sulfate, formic acid,

\* To whom correspondence should be addressed.

**Table I Base Polymerization Recipe**

|  |           |
|--|-----------|
| Vinyl acetate  | 250.00 g  |
| Vinol 205 (10%) <sup>a</sup>                               | 250.00 g  |
| H <sub>2</sub> O <sub>2</sub> (0.25%)                      | 25.00 g   |
| FeSO <sub>4</sub> ·7H <sub>2</sub> O solution <sup>b</sup> | 75.00 g   |
| Deionized H <sub>2</sub> O <sup>a</sup>                    | 400.00 g  |
| Total charge   | 1000.00 g |

<sup>a</sup> pH of V-205/H<sub>2</sub>O adjusted to 4.5.

<sup>b</sup> 0.5108 g FeSO<sub>4</sub>·7H<sub>2</sub>O diluted to 75.00 g.

and hydroquinone were all obtained from Fisher Scientific Company and used without further purification. The 3.4% active H<sub>2</sub>O<sub>2</sub> was further diluted with deionized water. The ferrous sulfate and hydroquinone were similarly diluted.

Polymerizations were conducted at 60°C in a 1-L semibatch reactor, with continuous hydrogen peroxide addition. The polymerization procedure started with an N<sub>2</sub> prepurge of the assembled reactor to ensure a proper seal and to minimize O<sub>2</sub> inhibition. The reactor was then charged with the pH-adjusted poly(vinyl alcohol) solution and vinyl acetate. The purge was continued while the reactor contents were agitated at 500 rpm and heated to 60°C. Forty-five minutes into the purge, a freshly-prepared FeSO<sub>4</sub> solution was added, and after an hour of purging, subsurface H<sub>2</sub>O<sub>2</sub> addition was begun. An N<sub>2</sub> blanket was maintained during the polymerization, and samples were removed as required. The polymerization was complete within 65 to 70 minutes. Mild agitation was maintained while disassembling the reactor to avoid skin formation.

Quenched intermediate and final latex samples were analyzed for monomer conversion and average particle size and distribution using gravimetric and light scattering techniques, respectively. Reactor samples, each weighing roughly 8 g, were quenched by immediate addition to a preweighed glass vial containing roughly 2 g of an aqueous 0.65% hydroquinone solution. Roughly 5 mL of the quenched latex solution was weighed into a preweighed aluminum pan and allowed to dry overnight in an ≈ 50°C oven for conversion measurements. The monomer conversion was then calculated from the dried sample weight, after correcting for the actual latex composition (e.g., H<sub>2</sub>O<sub>2</sub> added, previous samples removed, etc.). Average particle sizes and distributions were measured using the Malvern Autosizer IIc, an advanced system for particle size analysis by photon correlation spectroscopy. Although dynamic light scattering is only one of several operating principles exploited in commercial particle

size analyzers, the Malvern was chosen because of its fast analysis time and the resulting possibility of generating pseudo on-line data. Quenched reactor samples were simply diluted with filtered (dust-free) deionized water until the particle count was in the ideal range, as indicated by the instrumentation. The analysis option employed provided weight- and number-averaged particle diameters (for each sample) that were averages of 10 separate measurements (Aperture 200, temperature 25°C). This option eliminates measurements with low signal-to-noise ratios and/or less than 85% of the particles within a statistically-determined diameter range. Even with the repetitive measurements, the analysis time was impressive at less than 2 min per sample.

### Variable Specification

The model summary and solution requirements indicate that when six particle populations are required to predict the particle number concentration (i.e., nodes = 6), 53 variables must be specified, aside from the critical chain lengths for precipitation ( $n^*$  and  $n_g^*$ ) and the initial conditions for the ordinary differential equations. Less than half of these variables are provided by the polymerization recipe or literature estimates. The remaining variables are inferred or hypothesized based on probable mechanisms.

Variables calculated from the base recipe are summarized in Table II. The polymerization recipe and conditions fix the initial unreacted species concentrations and feed rates, the phase volumes, and the temperature and viscosity. The initial particle concentrations (not tabulated) are zero.

Variables estimated from the literature are summarized in Table III. The literature provides virtually no parameter values for polymerically-stabi-

**Table II Model Variables Specified by Polymerization Recipe**

| Variable | Value      | Units       |
|----------|------------|-------------|
| $F_{wi}$ | 2.4586E-03 | mol/L-aq    |
| $G_{wi}$ | 9.5743E-04 | mol/L-aq    |
| $I_f$    | 4.1649E-07 | mol/s       |
| $I_{wi}$ | 0.0000E+00 | mol/L-aq    |
| $M_i$    | 2.8257E+00 | mol/L-latex |
| $T$      | 3.3315E+02 | K           |
| $v_f$    | 5.6667E-06 | L/s         |
| $V_{di}$ | 2.8040E-01 | L-droplet   |
| $V_{ri}$ | 1.0277E+00 | L-latex     |
| $V_{wi}$ | 7.4733E-01 | L-aq        |
| $\eta$   | 4.6650E-01 | cp          |

**Table III Model Variables Estimated from the Literature**

| Variable       | Value      | Units              | Source                                    |
|----------------|------------|--------------------|---|
| $D_w$          | 1.0000E-06 | cm <sup>2</sup> /s | Pramojaney <sup>1</sup>                   |
| $k_d$          | 3.0294E+02 | L/mol-s            | Uri <sup>2</sup>                          |
| $k_{pw}$       | 3.7000E+03 | L/mol-s            | Rosen <sup>3</sup>                        |
| $k_{tre}$      | 3.5000E-03 | L/mol-s            | Dunn et al. <sup>4</sup>                  |
| $k_{trm}$      | 1.7500E-04 | L/mol-s            | Polymer Handbook                          |
| $k_{tw}$       | 3.8000E+08 | L/mol-s            | Polymer Handbook                          |
| $M_{ws}$       | 2.9000E-01 | mol/L-aq           | Vanderhoff <sup>5</sup>                   |
| $MW_m$         | 8.6090E+01 | g/gmol             | Polymer Handbook                          |
| $n^*$          | 6.0000E+01 | —                  | Pramojaney <sup>1</sup>                   |
| $n_g^*$        | 7.0000E+01 | —                  | Earhart <sup>6</sup>                      |
| $xdd$          | 1.5000E-01 | —                  | Warson, <sup>7</sup> Zollars <sup>8</sup> |
| $\rho_m$       | 8.0000E+02 | g/L                | Rosen <sup>3</sup>                        |
| $\rho_p$       | 1.1700E+03 | g/L                | Polymer Handbook                          |
| $\phi_{(xdd)}$ | 9.1318E-01 | —                  | Dunn and Taylor <sup>9</sup>              |
| $\chi$         | 3.8000E-01 | —                  | Klein et al. <sup>10</sup>                |

lized systems. However, since some parameters are probably more dependent upon the monomer type rather than the stabilizer, selected literature values for ionically-stabilized vinyl acetate systems are used as estimates in the subject system. A few of the estimates merit further discussion.

The vinyl acetate concentration in the aqueous phase at saturation ( $M_{ws}$ ) and the critical chain lengths for precipitation of the ungrafted and grafted oligomers ( $n^*$  and  $n_g^*$ ) all relate to the solubility of vinyl acetate (in some form) in water. One might expect the solubility of vinyl acetate in an aqueous poly(vinyl alcohol) solution to be greater than that in water because of the association between the acetate groups. However, as indicated in Table IV, Earhart<sup>6</sup> found that poly(vinyl alcohol) had no apparent effect on the water solubility of vinyl acetate under the subject conditions. Thus, no adjustment of literature  $M_{ws}$  and  $n^*$  values is required. Reported  $n^*$  values do, however, range from 50 to 300. Earhart<sup>6</sup> also determined that a graft poly(vinyl alcohol)-poly(vinyl acetate) copolymer remains water soluble up to 18% acetate content (82% hydro-

lyzed). This suggests that  $n_g^*$  is approximately 70 for the subject 88% hydrolyzed material.

The poly(vinyl alcohol) concentration also affects the conversion at which the monomer droplets disappear,  $xdd$ . Typically, due to its greater water solubility, vinyl acetate diffuses completely into the growing polymer particles very early in the reaction. Warson<sup>7</sup> and Zollars<sup>8</sup> measured the droplet disappearance at 15–20% conversion.

Up to the point of droplet disappearance, the aqueous phase is saturated with vinyl acetate and the volume fraction of monomer in the particles is constant at  $\phi_{(xdd)}$ . Given the vinyl acetate concentration in the aqueous phase at saturation ( $M_{ws}$ ), the concentration in the particles, and thus  $\phi_{(xdd)}$ , may be approximated from<sup>9</sup>

$$M_p = 13.7 M_w^2$$

where  $M_p$  and  $M_w$  are the wt % of vinyl acetate in the particle and aqueous phases, respectively. Netschey and Alexander<sup>12</sup> confirmed this distribution with analytical ultracentrifuge measurements at 20 and 40°C.

Variables inferred or hypothesized from literature discussions and probable mechanisms are summarized in Table V. The area covered by a single poly(vinyl alcohol) molecule, AG, is used to calculate the aqueous-phase poly(vinyl alcohol) concentration. Unlike conventional ionic surfactants, the adsorption of poly(vinyl alcohol) onto latex particles does not obey common adsorption isotherms such as the Langmuir model. At high surface coverage,<sup>13</sup> the poly(vinyl alcohol) molecules are compressed,

**Table IV Vinyl Acetate Solubility Data<sup>6</sup>**

|                                | Vinyl Acetate Water Solubility<br>(g/100 g H <sub>2</sub> O) |
|--------------------------------|--|
| Literature value <sup>11</sup> | 2.50   |
| DDI water                      | 2.47   |
| 10.0% Vinol 205                | 2.57   |
| 5.0% Vinol 205                 | 2.56   |
| 2.5% Vinol 205                 | 2.59   |

**Table V Model Variables Inferred or Hypothesized**

| Variable  | Value      | Units              |
|---|------------|--------------------|
| <i>AG</i>   | 1.8000E-13 | cm <sup>2</sup>    |
| <i>D<sub>pao</sub></i>                              | 2.8600E-08 | cm <sup>2</sup> /s |
| <i>eff</i>  | 0.0000E+00 | —                  |
| <i>f</i>  | 7.0000E-01 | —                  |
| <i>k<sub>iwe</sub></i>                              | 3.5000E-01 | L/mol-s            |
| <i>k'<sub>iwe</sub></i>                             | 3.5000E-02 | L/mol-s            |
| <i>k<sub>iwm</sub></i>                              | 3.7000E+05 | L/mol-s            |
| <i>k'<sub>iwm</sub></i>                             | 3.7000E+04 | L/mol-s            |
| <i>k<sub>pp</sub></i>                               | 3.7000E+03 | L/mol-s            |
| $\bar{n}$ , <i>P<sub>i</sub></i> , <i>i</i> < 5     | 1.0000E-01 | Rad/part           |
| $\bar{n}$ , <i>P<sub>i</sub></i> , <i>i</i> ≥ 5     | 5.0000E-01 | Rad/part           |
| Nodes   | 6.0000E+00 | —                  |
| <i>W<sub>ij</sub></i> , <i>i</i> or <i>j</i> = 1    | 1.0000E+00 | —                  |
| <i>W<sub>ij</sub></i> , <i>i</i> = <i>j</i> = nodes | 1.0000E+36 | —                  |
| <i>W<sub>ij</sub></i> , other                       | 3.3333E+03 | —                  |

entangled, or adsorbed in a multilayer fashion. Pramojaney<sup>1</sup> pointed out that the adsorptive area per molecule must be very large, e.g., the same order of magnitude as the surface area of a micelle, since a single poly(vinyl alcohol) molecule may function as a nucleation site for a primary particle in the same manner as a sodium lauryl sulfate micelle. Pramojaney<sup>1</sup> further estimated the adsorbed area per poly(vinyl alcohol) molecule (of the same nominal molecular weight used here) at 1800E-16 cm<sup>2</sup>/molecule.

Efficiency factors are used when calculating the primary initiator radical concentration and the average rate constant of radical capture by particles. In the former calculation, the initiation efficiency, *f*, expresses the fraction of *R*· radicals not consumed by side reactions. Values typically range from 0.7 to 1.0 (Vanderhoff<sup>5</sup>). The capture efficiency, *eff*, conceivably starts near 0.0 and increases to 1.0 as the particle concentration becomes large.

In the aqueous phase, both poly(vinyl alcohol) and vinyl acetate molecules are initiated by primary initiator radicals (*R*·) and desorbed primary monomeric radicals (*M*·<sub>1</sub>). Chern and Poehlein<sup>14</sup> investigated the kinetics of grafting in solution polymerization and suggested order of magnitude estimates for the various rate constants. Specifically, they presented the following ratios:

$$k'_{iwe}:k_{tre} \quad 10 : 1$$

$$k_{iwe}:k'_{iwe} \quad 10 : 1$$

$$k'_{iwm}:k_{pw} \quad 10 : 1$$

$$k_{iwm}:k_{pw} \quad 100 : 1$$

In all cases, the primary initiator radical is assumed more reactive than the desorbed primary monomeric species, thus  $k_{iwe} > k'_{iwe}$  and  $k_{iwm} > k'_{iwm}$ . Similarly, both species (*R*· and *M*·<sub>1</sub>) are more reactive than a poly(vinyl acetate) oligomer (*RM*·<sub>*i*</sub>), so  $k_{iwm}$ ,  $k'_{iwm} > k_{pw}$  and  $k_{iwe}$ ,  $k'_{iwe} > k_{tre}$ . Chern and Poehlein<sup>14</sup> noted that their model was somewhat insensitive to the  $k_{iwm} : k_{pw}$  ratio.

Considerable sensitivity is expected, however, to the average number of radicals per particle,  $\bar{n}$ . Vinyl acetate systems are typically characterized as Smith-Ewart Case 1, e.g.,  $\bar{n} < 0.5$ , because vinyl acetate is relatively soluble in water and transfers readily with poly(vinyl acetate) oligomers. The resulting monomeric radicals are very mobile, easily traversing the particle surface during much of the polymerization. In poly(vinyl alcohol)-stabilized systems, however, the high viscosity of the thick hydrate layer and chain transfer of growing poly(vinyl acetate) chains to poly(vinyl alcohol) instead of vinyl acetate may significantly limit free radical mobility. It is thus conceivable that  $\bar{n}$  is closer to 0.5 for polymerically-stabilized particles.

Vanderhoff<sup>5</sup> suggested that for an ionically-stabilized vinyl acetate system, particles consisting of five or more primary particles are generally stable and grow by polymerization and capture of particles of subcritical stability, i.e., < 5 primary particles. Vanderhoff's suggestions are based on surface charge considerations and are therefore not directly applicable to the subject system. Nonetheless, they offer a starting point for model simulations. Therefore, it is assumed that particles in populations less than *P*<sub>5</sub> contain, on the average, 0.1 radical per particle while the larger, stable particles contain 0.5 radical per particle. For all populations, theory correctly predicts that  $\bar{n}$  increases with increased conversion, but, for this system, more unknown parameters are introduced. The added model structure does not appear to justify the accompanying uncertainty.

Another key parameter, nodes, indicates the number of particle populations required to predict the experimental particle concentration. While there is little guidance in choosing this parameter, the experimental profile obviously depends on the detection range of the particle size analyzer. When dynamic laser light scattering is employed via the Malvern Autosizer, the lower detection limit is nominally 3 nm. For a critical chain length, *n*<sup>\*</sup>, of 60–70, Vanderhoff<sup>5</sup> suggested a primary particle diameter of roughly 2.5 nm. Thus, a spherical particle consisting of roughly two primary particles should

be experimentally detectable, suggesting that  $P = P_2 + \dots + P_{nodes}$ . Detection is obviously affected, however, by the presence of larger particles.

Hiemenz<sup>15</sup> offers some insight in choosing the Fuchs stability ratios,  $W_{ij}$ , which increase with the relative stability of species  $i$  and  $j$ . For simplicity, assume that species  $i$  and  $j$  either flocculate very quickly ( $W_{ij}$  small, 1.0), flocculate more slowly ( $W_{ij}$  intermediate), or remain separate ( $W_{ij}$  large,  $1.0E + 36$ ). Hiemenz<sup>15</sup> stated that a Fuchs stability ratio of  $10^4$  corresponds to overcoming a potential energy barrier of roughly 15 kT. He further noted that polymerically stabilized systems slowly flocculate at potential energies of roughly 5 kT, suggesting a Fuchs stability ratio of about 3333. Therefore, assume that if either  $i$  or  $j$  is 1, i.e., a primary particle is involved, the particles flocculate very quickly ( $W_{ij} = 1$ ), but there is negligible homogeneous flocculation within the lumped population, i.e.,  $W_{ij} = 1.0E + 36$  when  $i = j = nodes$ . Other particles flocculate at the slower rate characterizing polymerically stabilized systems ( $W_{ij} = 3333$ ).

### Model Sensitivity

Considering the large number of unspecified model parameters, a brief discussion of model sensitivity is appropriate prior to comparing predictions with experimental results. In lieu of a rigorous statistical sensitivity analysis, consider the sensitivity of model predictions to changes in single key parameters. Of the 53 unspecified variables, 19 are either specified by the polymerization recipe or known with reasonable certainty from the literature. The remaining 34 (including the 21 Fuchs stability ratios) are less certain, subject to a range of literature values, or no estimates at all.

Over the ranges tested, model predictions of measurable variables exhibited sensitivity to nine variables,  $n^*$ ,  $eff$ ,  $W_{ij}$ ,  $k_{pp}$ ,  $\bar{n}$ ,  $k_{pw}$ ,  $f$ ,  $k_{tw}$ , and  $nodes$ , most affecting either primary ungrafted particle nucleation or flocculation kinetics. Predictions were relatively insensitive to variables affecting poly(vinyl alcohol) grafting reactions and the resulting primary grafted particle concentration. Extreme sensitivity was noted to  $n^*$ ,  $eff$ , and  $W_{ij}$  in the case of  $P$  predictions, and  $k_{pp}$  and  $\bar{n}$  in the case of  $x$  predictions. Assuming systems characterized by relatively water-soluble monomers with high propagation constants have capture efficiencies near 0 until late in the polymerization, only  $n^*$ ,  $W_{ij}$ ,  $k_{pp}$ , and  $\bar{n}$  remain as key adjustable parameters. Of these four, literature guidance is generally available for three, namely  $n^*$ ,  $k_{pp}$ , and  $\bar{n}$ , leaving  $W_{ij}$  as the major challenge.

The particle concentration is very sensitive to the Fuchs stability ratios (Fig. 1). In Figure 1, the base condition assumes that

1.  $W_{ij} = 1.0$  if  $i$  or  $j$  is a primary particle (fast flocculation);
2.  $W_{ij} = 1.0E + 36$  if both  $i$  and  $j$  are in the lumped population (minimal flocculation); and
3.  $W_{ij} = 3333$  for all other  $i, j$  combinations (slower flocculation). Case A in Figure 1 assumes that all particles not protected by a steric layer flocculate quickly ( $W_{ij} = 1.0$ ), while protected particles flocculate at the slower rate characterizing sterically stabilized systems ( $W_{ij} = 3333$ ). Returning to Vanderhoff's<sup>5</sup> suggestion that particles in populations less than  $P_5$  are unstable, Case A may be restated as  $W_{ij} = 1.0$  if  $i$  or  $j$  is less than 5, and  $W_{ij} = 3333$  for all other  $i, j$  combinations. Clearly, this significantly increases flocculation among nonprimary particle populations and allows homogeneous flocculation within the lumped population, decreasing  $P$ .

### Simulation Results

Model simulations of the base recipe and reaction conditions were generated using the previously tabulated variables. As illustrated in the following figures, model predictions agree reasonably well with author-generated data and provide further insight into the polymerization mechanism. For discussion purposes, consider first the particle number profile, and then the prediction of other aqueous-phase and particle-related parameters, and measured variables.

As expected, the particle number increases throughout much of the polymerization, leveling only after roughly 80% conversion (Fig. 2). This

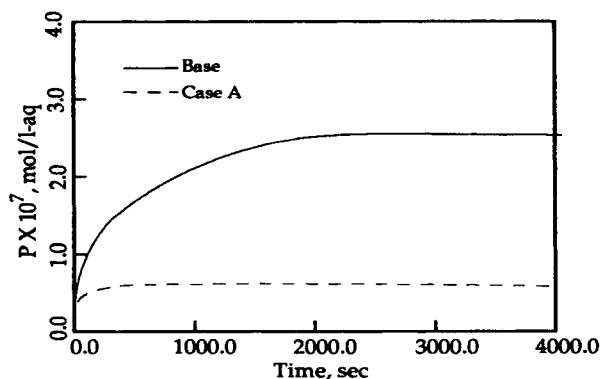
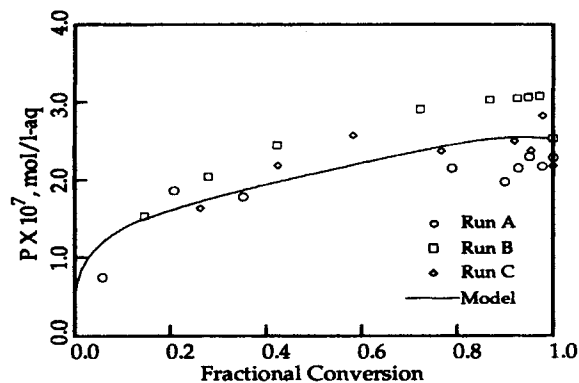


Figure 1 Effect of  $W_{ij}$  on the stable particle concentration.



**Figure 2** Model prediction of measurable particle concentration for duplicate base recipe runs *A*, *B*, *C*.

profile supports the mechanistic hypothesis of continuous homogeneous nucleation. Primary ungrafted particles are not included in this concentration, and thus the expected virtually instantaneous population explosion at the beginning of the reaction is not depicted in Figure 2. However, the concentration of primary particles nucleated from grafted poly(vinyl alcohol) molecules is assumed stable from the onset and is therefore included in the Figure 2 profile. Indeed, both grafted and ungrafted primary particle concentrations explode initially (Figs. 3, 4), but the number of grafted particles, while sustained through inherent stability, is much less than the number of ungrafted particles. The model then suggests that the measurable particle concentration increases primarily via flocculation of primary particles nucleated from ungrafted poly(vinyl acetate) oligomers.

Delving further into the nucleation mechanism, note that the preponderance of ungrafted versus grafted primary particles mostly reflects the dependence of the latter on the smaller concentration of

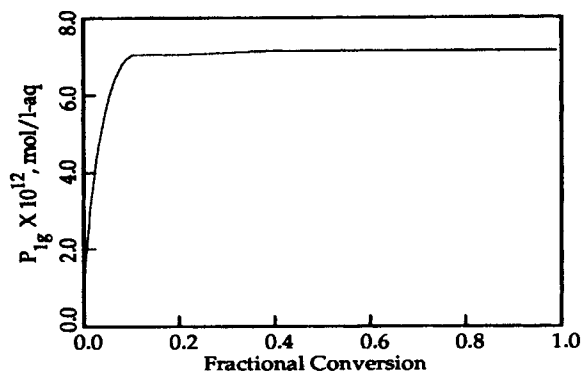


**Figure 3** Model prediction of grafted primary particle concentration (base recipe).

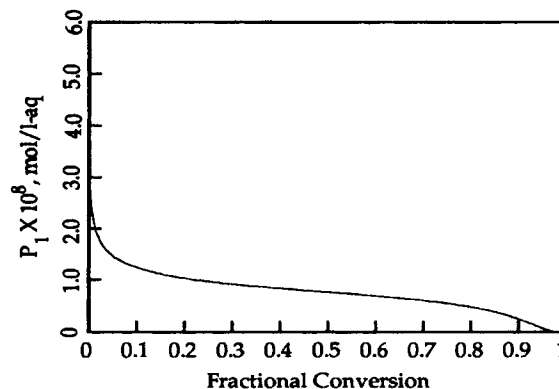


**Figure 4** Model prediction of ungrafted primary particle concentration (base recipe).

primary grafted initiator radicals,  $[G\cdot]$ , rather than  $[R\cdot]$ .  $[G\cdot]$  is on the order of  $10^{-17}$  mol/L-aq, and decreases with  $G_w$ , while  $[R\cdot]$  is on the order of  $10^{-11}$  mol/L-aq and is constant or increasing throughout the polymerization. Recall,

$$[RM\cdot_i] = \alpha_{Mp}^{i-1} [RM\cdot_1] \quad \text{where}$$

$$[RM\cdot_1] = \alpha_{Mp} \left( \frac{k_{iwm}}{k_{pw}} \right) [R\cdot]$$

$$[GM\cdot_i] = \alpha_{GMp}^{i-1} [GM\cdot_1] \quad \text{where}$$

$$[GM\cdot_1] = \alpha_{GMp} [G\cdot].$$

Grafted radicals,  $G\cdot$ , are formed only via chain transfer of existing radical species to poly(vinyl alcohol) molecules, while ungrafted  $R\cdot$  radicals are formed directly from the redox reaction. Since neither the reductant ( $F_w$ ) nor the oxidant ( $I_w$ ) is in limiting quantity ( $I_w$  is actually in excess), and the rate constant  $k_d$  is larger than any of the chain transfer constants,  $[R\cdot]$  is orders of magnitude larger than  $[G\cdot]$ . In addition,  $R\cdot$  radicals propagate more rapidly than  $G\cdot$  radicals ( $k_{iwm} > k_{pw}$ ), further increasing  $[RM\cdot_1]$  relative to  $[GM\cdot_1]$ , and grafted oligomers propagate to a larger critical chain length before precipitation, further decreasing  $[GM\cdot_{n^*-1}]$  relative to  $[RM\cdot_{n^*-1}]$ . Finally, recall the propagation probabilities for the ungrafted and grafted species,  $\alpha_{Mp}$  and  $\alpha_{GMp}$ .

$$\alpha_{Mp} = \frac{k_{pw}M_w}{k_{pw}M_w + k_{trm}M_w + k_{tre}G_w + k_{tw}[R\cdot_w] + k_cP}$$

$$\alpha_{GMp} = \frac{k_{pw}M_w}{k_{pw}M_w + k_{trm}M_w + k_{tre}G_w + k_{tw}([RM\cdot] + [M\cdot])}$$

For this base case, these probabilities are identical since the capture efficiency is assumed to be zero, and the grafted oligomers contribute negligibly to the total aqueous-phase radical concentration ( $[GM\cdot]$  is on the order of  $10^{-15}$  mol/L-aq, while  $[R\cdot_w]$  is on the order of  $10^{-8}$  mol/L-aq). Thus, for these conditions and assumptions, the model appears consistent in predicting the lesser importance of grafting in particle nucleation.

As expected, the conversion profile (Figure 5) is qualitatively similar to those obtained in ionically-stabilized systems, suggesting three stages of polymerization: the rate accelerates initially, is relatively constant for a period, and then decreases as the vinyl acetate is depleted. The stages are not as distinct, however, as those commonly observed in batch systems. Also, as assumed, unmeasurable particle and aqueous-phase conversion was negligible compared with measured particle conversion. Using this assumption, the average unswollen particle diameter profile (Fig. 6) is based on the measurable particle concentration. As expected, the diameter increases steadily, leveling at high conversion.

In summary, the model reasonably predicts the experimental data and suggests, for these base conditions and assumptions, that grafting is less important in the homogeneous particle nucleation mechanism. This is consistent with recent findings of Kroener and Dimonie,<sup>16</sup> who noted that under high solids conditions (high monomer concentration), the primary particle formation is caused by homogeneous nucleation of the vinyl acetate oligomers. While some poly(vinyl alcohol) is grafted, they speculate that this may be the primary nucleation mechanism at low monomer concentrations.

The base semibatch simulations may be extended to further illustrate the particle nucleation and grafting trends accompanying recipe changes. Lit-

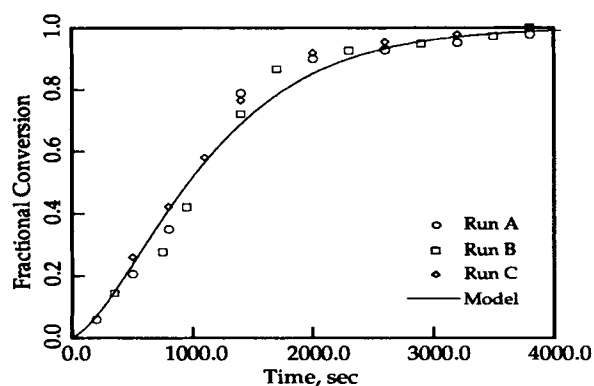


**Figure 5** Model prediction of fractional conversion for duplicate base recipe runs A, B, C.

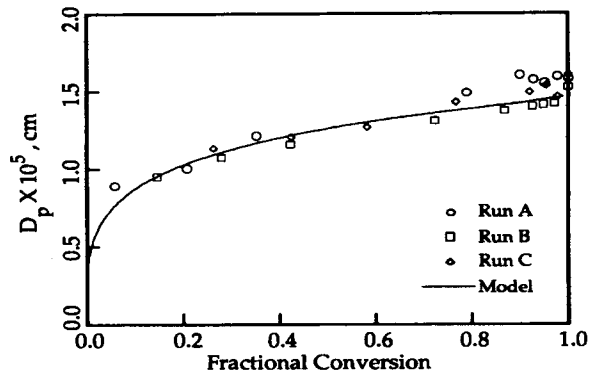


**Figure 6** Model prediction of average unswollen particle diameter for duplicate base recipe runs A, B, C.

erature reports and mechanism considerations suggest that the relative concentrations of poly(vinyl alcohol), vinyl acetate, and initiator are important parameters of the grafting reaction. Indeed, simulations of variations in the base semibatch (initiator added during polymerization) recipe indicate that independent increases in the vinyl acetate, poly(vinyl alcohol), and initiator levels all increase the primary grafted particle population. It is unlikely, however, that this population exceeds the ungrafted counterpart under most commercial polymerization conditions.

Other poly(vinyl alcohol) characteristics specifically accommodated by the model also affect the grafted primary particle concentration. Namely, increasing either the molecular weight or hydrolysis level decreases  $P_{1g}$ . Increasing the molecular weight effectively decreases  $G_{wi}$  and increases  $n_g^*$ , as more vinyl acetate molecules must be added to render the grafted chain insoluble. Both of these factors tend to decrease  $P_{1g}$ .

The critical chain length for precipitation also increases with the poly(vinyl alcohol) hydrolysis level since the initial water-solubility is increased. Thus, an increased nominal hydrolysis level also decreases  $P_{1g}$ . Other more subtle intramolecular poly(vinyl alcohol) characteristics (e.g., blockiness) undoubtedly affect the grafting reaction and the resulting primary particle concentration. This is most directly reflected in  $k_{iwe}$  or  $k'_{iwe}$ , the rate constants characterizing the reactions yielding the  $G\cdot$  species. Previous analysis suggests, however, that, unlike the  $P_{1g}$  profiles, the predicted  $P$  profiles are relatively unaffected by order of magnitude changes in  $k_{iwe}$  or  $k'_{iwe}$ .

Overall, the semibatch simulations suggest that grafting during particle nucleation is less important in typical commercial recipes. Consider, however,

that the experimental conditions used by Hartley<sup>17</sup> reportedly yielded a significant graft copolymer concentration during nucleation. Here, the monomer and catalyst were added to a buffered poly(vinyl alcohol) solution, constituting a semibatch configuration with both initiator and monomer delays. The subject model assumes that the aqueous phase is saturated with monomer at the onset of polymerization, and thus does not explicitly accommodate Hartley's<sup>17</sup> conditions. However, these conditions may be approached in batch simulations by decreasing the monomer and initiator with a fixed poly(vinyl alcohol) concentration. In the limit of very low monomer concentrations, with a fixed high poly(vinyl alcohol) concentration, the initiator molecules would activate more grafting sites on the poly(vinyl alcohol) chains and thus increase the potential contribution of grafting to particle nucleation.

Although the contribution of grafting to particle nucleation is potentially increased at low monomer and high poly(vinyl alcohol) concentrations, very unusual, perhaps unachievable, conditions would be required for the grafted population to actually exceed the ungrafted primary particle concentration. In the base recipe, the initial molar ratio of vinyl acetate to poly(vinyl alcohol) is roughly 2950 : 1. Apart from the previously discussed kinetic considerations, initiation of a vinyl acetate molecule is clearly favored over chain transfer to a poly(vinyl alcohol) molecule. Even with the lowest molecular weight poly(vinyl alcohol) commercially available (degree of polymerization 500–700), excessively high concentrations would be required to achieve a more equitable molar ratio, resulting in intolerably high latex viscosities. The semibatch addition of both initiator and vinyl acetate lessens the inequity in molar

concentrations, but the vinyl acetate addition rate must still be very low (cf. initiator rate) to overcome the kinetically-favored initiation reaction. The low monomer concentration would probably lower the reaction rate to an unacceptable level. Lastly, relaxing the simplifying assumption of one grafting site per poly(vinyl alcohol) molecule would also lessen the molar inequity, but prohibitively low monomer concentrations would still be required.

### Batch Simulations

Although the literature does not provide experimental data for the exact subject recipe, O'Donnell et al.<sup>18</sup> and Pramojaney<sup>1</sup> present conversion data for the batch polymerization of vinyl acetate stabilized with poly(vinyl alcohol) and initiated with potassium persulfate (KPS) (Table VI). In addition to the altered initiation kinetics associated with thermal initiation (as opposed to a redox system), the batch configuration results in higher initiator concentrations. As discussed below, with appropriate variable adjustments, model predictions agree well with the experimental data and again suggest that (under these conditions) grafting is less important during particle nucleation.

First, prior to discussing either data set in detail, note that with a thermal initiator, the decomposition reaction becomes

$$I \xrightarrow{k_d} 2R.$$

and  $F_w$  and associated expressions become meaningless. Assuming first-order kinetics and batch operation, model equations become

**Table VI Comparison of Base Recipe and Process with Those of O'Donnell et al.<sup>18</sup> and Pramojaney<sup>1</sup>**

|                      | Base   | O'Donnell et al. <sup>18</sup> | Pramojaney <sup>1</sup> |
|----------------------|--|--------------------------------|-------------------------|
| VAc solids (%)       | 25.0   | 20.0                           | 28.8                    |
| PVOH                 |  |                                |                         |
| Percent Hydrolyzed   | 88   | 88                             | 88                      |
| Molecular wt         | 34,940   | 78,000                         | 48,000                  |
| Percent based on VAc | 10.0   | 4.0–8.0                        | 5.0–10.0                |
| Initiator            |  |                                |                         |
| Type                 | H <sub>2</sub> O <sub>2</sub> /FeSO <sub>4</sub> | KPS                            | KPS                     |
| Percent based on VAc | 0.025  | 0.04–0.20                      | 0.35–2.0                |
| Process              |  |                                |                         |
| Configuration        | Semibatch  | Batch                          | Batch                   |
| Temperature (°C)     | 60.0   | 70.0                           | 50.0                    |



$$\frac{dI_w}{dt} = -k_d I_w$$

$$[R\cdot] = \frac{2fk_d I_w}{k_{iwm}M_w + k_{iwe}G_w}$$

While the literature provides  $k_d$  values for KPS in water and NaOH solutions at various temperatures, it is known that this decomposition is significantly accelerated in the presence of poly(vinyl alcohol)<sup>4,19-21</sup> and ester monomers such as vinyl acetate.<sup>22</sup> In fact, according to Gulbekian and Reynolds,<sup>21</sup> the rate of KPS decomposition in the presence of poly(vinyl alcohol) is proportional to  $I_w G_w^{0.5}$ . While it is uncertain to what extent poly(vinyl alcohol) grafted to the particle surface may still influence the decomposition of KPS, a significant number of hydroxy groups do extend into the aqueous phase. This suggests a proportionality to  $G_{wi}$  rather than  $G_w$ , and the above equations become

$$\frac{dI_w}{dt} = -k_d I_w G_{wi}^{0.5}$$

$$[R\cdot] = \frac{2fk_d I_w G_{wi}^{0.5}}{k_{iwm}M_w + k_{iwe}G_w}$$

Rather than further extending the dependence of  $(dI_w)/dt$  to include  $M_w$  as well,  $k_d$  is viewed as an adjustable parameter, and increased to reflect further enhanced KPS decomposition.

In addition to  $k_d$ ,  $\bar{n}$  is chosen as a second adjustable parameter. The batch configuration, and resulting higher overall initiator concentrations, suggests possible higher  $\bar{n}$  and/or  $P$  levels. If use of an average  $\bar{n}$  [i.e.,  $\bar{n} \neq f(x)$ ] does not provide an acceptable fit, a simple dependence of  $\bar{n}$  on  $\phi$  ( $\bar{n} = (A/\phi) + B$ , where  $A$  and  $B$  are adjustable parameters) is suggested. This dependence is intuitively justified by considering equations presented by Song,<sup>23</sup> expressing  $\bar{n}$  as a function of the Ugelstad parameters  $\alpha'$ ,  $m$ , and  $Y$ . The equations yield results in agreement with those obtained from Ugelstad and Hansen's<sup>24</sup> continued fraction form, a simplification of the rigorous radical balance approach. For this system, the equations reduce to  $\bar{n} = 0.5$ , the value successfully used during simulations of the base recipe. As the polymerization progresses, and the stable, poly(vinyl alcohol)-protected particle population increases,  $\bar{n}$  may increase. It is reasonable to assume that  $\bar{n}$  is more strongly affected by reactions within the particle since the thick hydrate layer could significantly limit free radical mobility. Furthermore,

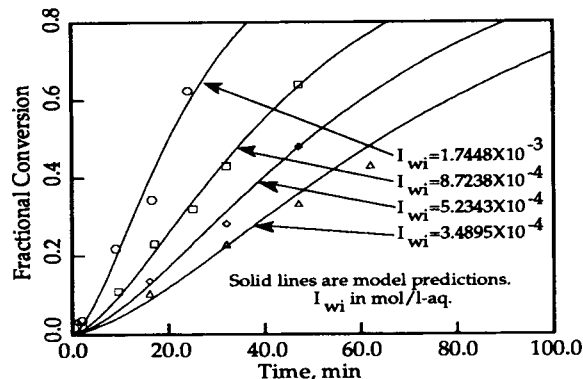


Figure 7 Model predictions of conversion for O'Donnell initiator series.

intraparticle reaction rate constants eventually reflect diffusion limitations (due to increased viscosity) and correlate with  $\phi$ , leading to an expected dominant  $\bar{n} - \phi$  dependence.

Now, consider the data of O'Donnell et al.<sup>18</sup> In addition to the batch configuration and KPS initiator, O'Donnell's polymerizations were conducted at a slightly lower solids level and higher temperature compared to the base recipe. The poly(vinyl alcohol) was of the same nominal hydrolysis level, but of higher molecular weight. O'Donnell reported data from two experimental series. In one, the poly(vinyl alcohol) was fixed at  $\approx 4\%$  and the initiator varied from 0.04 to 0.20%, while in the other, the initiator level was fixed at 0.10% and the poly(vinyl alcohol) varied from 4 to 8% (Table VI). (All percentages are wt % based on vinyl acetate.)

Model predictions for the O'Donnell initiator series are shown in Table VII and Figure 7. The average  $\bar{n}$  values listed in Table VII provide an acceptable fit between the model and experimental conversion data. The expected trend of decreased reaction time (increased reaction rate) with increased initiator level is confirmed. The increased reaction rate results primarily from increases in  $\bar{n}$  and  $P$ . Higher initiator concentrations increase the nucleation of primary particles and the subsequent stable particle population. The primary ungrafted population peaks early in the reaction, but still overwhelms the primary grafted population, again suggesting the relative insignificance of grafting during nucleation under these conditions.

Model predictions for the O'Donnell poly(vinyl alcohol) series are shown in Table VIII and Figure 8. Again, even when the poly(vinyl alcohol) concentration is doubled, the population of grafted primary particles is small compared to the ungrafted population. As in the initiator series, the reaction

**Table VII Model Parameters and Predictions for O'Donnell et al.<sup>18</sup> Initiator (KPS) Series**

| Adjusted Variables  |           | Predicted Level at $x = 0.8$ |            |
|---------------------|-----------|------------------------------|------------|
| $I_{wi}$ (mol/L-aq) | $\bar{n}$ | $P$ (mol/L-aq)               | $D_p$ (cm) |
| 3.4895E-04          | 0.55      | 3.4878E-08                   | 2.3105E-05 |
| 5.2343E-04          | 0.60      | 4.4363E-08                   | 2.2101E-05 |
| 8.7238E-04          | 0.65      | 5.6284E-08                   | 2.0389E-05 |
| 1.7448E-03          | 0.90      | 7.3501E-08                   | 1.8653E-05 |

$$G_{wi} = 1.2088E-04.$$

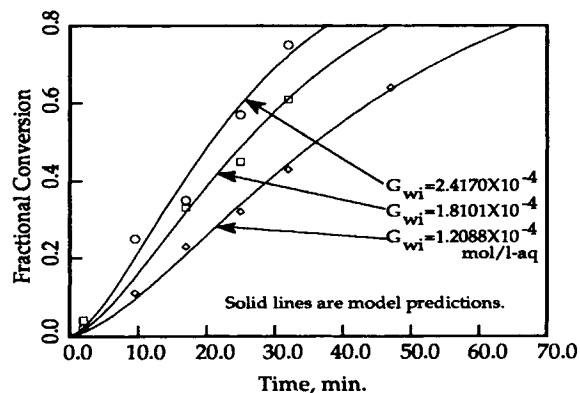
time decreases with increased poly(vinyl alcohol) level. Here, however, the increase in  $P$  is less pronounced, and the increase in  $\bar{n}$  more pronounced. Higher poly(vinyl alcohol) concentrations further accelerate the initiator decomposition and thus increase the primary particle concentration. The increase is less than that observed with an initiator increase since initiator decomposition is assumed proportional to  $I_w G_{wi}^{0.5}$ . The  $\bar{n}$  values required for an acceptable model/data fit increase with poly(vinyl alcohol) concentration, most probably reflecting a thicker hydrate layer (around the particles) and further free radical mobility restrictions.

Pramojaney<sup>1</sup> also utilized the batch configuration and KPS initiator, but conducted polymerizations at a higher solids level and lower temperature compared to the base recipe. The poly(vinyl alcohol) was of the same nominal hydrolysis level, but slightly higher in molecular weight. Like O'Donnell et al.,<sup>18</sup> Pramojaney<sup>1</sup> reported data from two experimental series. In one, the poly(vinyl alcohol) level was fixed at 7.4% and the initiator varied from 0.35 to 2.0%, while in the other, the initiator level was fixed at 0.67% and the poly(vinyl alcohol) varied from 5 to 10% (Table VI). (All percentages are wt % based on vinyl acetate.)

**Table VIII Model Parameters and Predictions for O'Donnell et al.<sup>18</sup> Poly(Vinyl Alcohol) Series**

| Adjusted Variables  |           | Predicted Level at $x = 0.8$ |            |
|---------------------|-----------|------------------------------|------------|
| $G_{wi}$ (mol/L-aq) | $\bar{n}$ | $P$ (mol/L-aq)               | $D_p$ (cm) |
| 1.2088E-04          | 0.65      | 5.6284E-08                   | 2.0389E-05 |
| 1.8101E-04          | 0.90      | 5.7395E-08                   | 2.0245E-05 |
| 2.4170E-04          | 1.10      | 5.8721E-08                   | 2.0104E-05 |

$$I_{wi} = 8.7238E-04.$$

**Figure 8** Model predictions of conversion for O'Donnell poly(vinyl alcohol) series.

Model predictions for the Pramojaney<sup>1</sup> initiator series are shown in Table IX and Figure 9. The  $A$ ,  $B$  values listed in Table IX provide an acceptable fit between the model and experimental conversion data (Fig. 9). The purely empirical  $A$ ,  $B$  values are determined by calculating the  $\bar{n}$  profile required to fit the experimental data, and then fitting the curve to the  $\bar{n} = (A\phi) + B$  form. At very high conversions, the calculated  $\bar{n}$  decreases to accommodate the lower reaction rate. The lower reaction rate, however, reflects a decrease in  $k_{pp}$  (monomer concentration is directly accounted for) rather than a decrease in  $\bar{n}$ . Since the model does not account for a decrease in  $k_{pp}$  at high conversions, and the  $\bar{n} - \phi$  correlation correctly predicts a continued  $\bar{n}$  increase, the model/data fit deteriorates at very high (> 95%) conversions. For all initiator levels,  $\bar{n}$  varies between 0.5 and 1.0 during most of the polymerization, and then increases by an order of magnitude during the last phase. This trend agrees with numerous literature investigations, including those of Song,<sup>23</sup> that predict an eventual increase in  $\bar{n}$  with conversion (less free radical escape), even in conventional vinyl acetate systems.

Model predictions for the Pramojaney<sup>1</sup> poly(vinyl alcohol) series are shown in Table X and Figure 10. Here, with no further  $\bar{n}$  adjustment, the model predicts a slight, and apparently experimentally undetectable, increase in reaction rate with increased poly(vinyl alcohol) level (Fig. 10). The reaction rate increase is precipitated by an increase in  $P$ , which results from an increase in the primary particle population. In addition to increasing the initiator decomposition, and thus particle nucleation, increasing the poly(vinyl alcohol) concentration directly increases the grafted primary particle

**Table IX Model Parameters and Predictions for Pramojaney<sup>1</sup> Initiator (KPS) Series**

| $I_{wi}$ (mol/L-aq) | Adjusted Variables |          | Predicted Level at $x = 0.95$ |            |
|---------------------|--------------------|----------|-------------------------------|------------|
|                     | $A$                | $B$      | $P$ (mol/L-aq)                | $D_p$ (cm) |
| 4.7319E-03          | 0.26816            | -0.06822 | 1.1959E-07                    | 1.9769E-05 |
| 9.4637E-03          | 0.21700            | +0.21800 | 1.5770E-07                    | 1.8035E-05 |
| 1.8927E-02          | 0.24102            | +0.31445 | 2.0997E-07                    | 1.6378E-05 |
| 2.8391E-02          | 0.58261            | -0.10873 | 2.3321E-07                    | 1.5799E-05 |

$$G_{wi} = 5.9154E-04.$$

population. This population remains small, however, compared to the ungrafted counterpart.

Prior to ending this discussion of literature data simulations, consider briefly the  $\bar{n}$  adjustments required to achieve acceptable model/data fits. Specifically, at lower initiator concentrations, i.e., the O'Donnell<sup>18</sup> data, an average  $\bar{n}$  suffices, but further adjustment is required when the poly(vinyl alcohol) level is altered. At higher initiator concentrations, i.e., the Pramojaney data, an empirical  $\bar{n} - \phi$  correlation is required, but no further adjustment is needed when the poly(vinyl alcohol) level is altered. The further increase of  $\bar{n}$  with poly(vinyl alcohol) concentration presumably reflects a thicker hydrate layer and the resulting decreased free radical mobility. As indicated in Table XI, for a given particle surface coverage, i.e., moles poly(vinyl alcohol)/particle, the  $\bar{n}$  range is rather consistent between both data sets, lending credibility to the  $\bar{n}$  adjustment methods.

In summary, with appropriate reaction variables and reasonable use of  $k_d$  and  $\bar{n}$  as adjustable parameters, model predictions agree well with the batch, thermal-initiation conversion data of O'Donnell et

al.<sup>18</sup> and Pramojaney.<sup>1</sup> The reaction rate is increased by increases in either initiator or poly(vinyl alcohol) concentration, as both increase  $P$ , the stable particle population, and/or  $\bar{n}$ . As expected, the grafted primary particle population also increases, but still wanes in comparison to the ungrafted counterpart, suggesting that grafting is less important during particle nucleation under these conditions.

## CONCLUSIONS

Model utility may be viewed from two perspectives: (1), utility in studying particle nucleation, and (2), application to potential commercial polymerization control schemes. While some kinetic constants are uncertain, the present model accounts for the chemical reactions in the homogeneous nucleation mechanism and is therefore very useful in predicting the relative importance of poly(vinyl alcohol) grafting during nucleation. Obviously, the stable particle population depends not only on how many particles are nucleated, but also on the subsequent stability of these primary particles. The model admittedly oversimplifies the stability issue by assuming three levels of flocculation—fast, slow, and in-

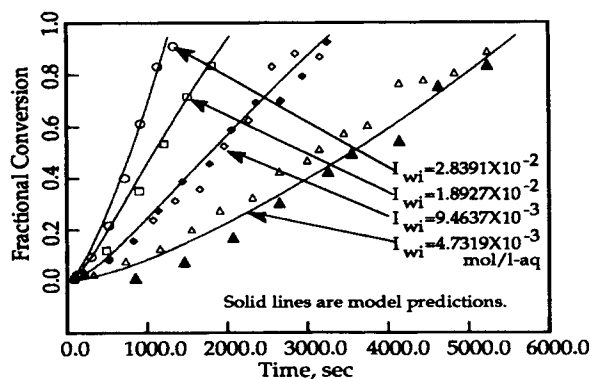


**Figure 9** Model predictions of conversion for Pramojaney initiator series.

**Table X Model Parameters and Predictions for Pramojaney<sup>1</sup> Poly(Vinyl Alcohol) Series**

| Adjusted Variable   | Predicted Level at $x = 0.8$ |            |
|---------------------|------------------------------|------------|
| $G_{wi}$ (mol/L-aq) | $P$ (mol/L-aq)               | $D_p$ (cm) |
| 3.9437E-04          | 1.4303E-07                   | 1.8622E-05 |
| 5.9154E-04          | 1.5770E-07                   | 1.8035E-05 |
| 7.8874E-04          | 1.6888E-07                   | 1.7618E-05 |

$$I_{wi} = 9.4637E-03.$$

intermediate—with little theoretical basis. A thorough thermodynamic treatment would require use of the HVO theory (developed by Hesselink, Vrij, and Overbeek) to generate stability diagrams depicting latex stability as a function of the change in free energy when polymer-covered particles approach one another.

The application of the theory, however, requires detailed poly(vinyl alcohol) configuration properties, such as the number of tails (or loops) per unit area and the mean square end-to-end distance each tail would have in solution. Realistically, even the particle surface area covered per poly(vinyl alcohol) molecule varies in a controlled laboratory system, and most certainly in commercial manufacturing processes. Thus, although the model accommodates flocculation kinetics in stable particle population calculations, it also relies on an empirical rule-of-thumb for the level of poly(vinyl alcohol) required for stability. Namely, most commercial latex recipes tolerate 5–20 wt % poly(vinyl alcohol) based on monomer. The lower 5% limit reflects the minimum stability requirement, while the upper 20% limit reflects latex viscosity limitations.

Model use of simplified flocculation kinetics and an empirical poly(vinyl alcohol) level range limits application in sophisticated control schemes, since the model structure does not directly relate the poly(vinyl alcohol) and stable particle concentrations. However, despite the simplifications, the model predicts semibatch and batch experimental data trends with reasonable accuracy and suggests that, when the molar ratio of vinyl acetate to poly(vinyl alcohol) is high, grafted primary particles do not contribute significantly to the total primary particle concentration. Note however, that although grafting does not play a significant role during par-

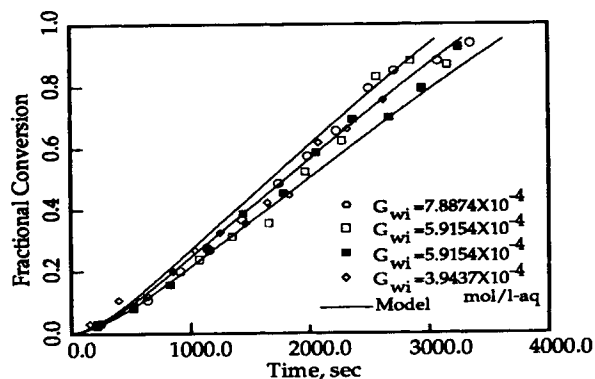


Figure 10 Model predictions of conversion for Pramojaney poly(vinyl alcohol) series.

Table XI Particle Surface Coverage vs.  $\bar{n}$

| O'Donnell et al. <sup>18</sup> |           | Pramojaney <sup>1</sup>      |             |
|--------------------------------|-----------|------------------------------|-------------|
| $G_{wi}/N$<br>(mol/particle)   | $\bar{n}$ | $G_{wi}/N$<br>(mol/particle) | $\bar{n}^a$ |
| 3.6063E-21                     | 0.65      | 4.5914E-21                   | 0.5–1.5     |
| 5.2765E-21                     | 0.90      | 6.2401E-21                   | 0.5–1.5     |
| 6.8623E-21                     | 1.10      | 7.7628E-21                   | 0.5–1.5     |

<sup>a</sup> Range from 0 to 80% conversion.

ticle nucleation, numerous investigators have reported that the grafting of poly(vinyl acetate) onto partially hydrolyzed poly(vinyl alcohol) enhances latex stability, and the poly(vinyl alcohol) is chemically bound to the particle surface in the final latex. This suggests that chemical grafting may follow physical adsorption.

## REFERENCES

1. N. Pramojaney, Ph.D. thesis, Lehigh University, 1982.
2. N. Uri, *Chemical Reviews*, **50**, 375 (1952).
3. S. L. Rosen, *Fundamental Principles of Polymeric Materials*, Barnes & Noble, Savage, MD, 1971, p. 143.
4. A. S. Dunn, C. J. Tonge, and S. A. B. Anabtawi, in *Emulsion Polymerization: ACS Symp. Ser. No. 24*, I. Piirma and J. L. Gardon, Eds., ACS, Washington, D.C., 1976, p. 24.
5. J. W. Vanderhoff, *J. Polym. Sci., Polym. Symp.*, **72**, 161–198 (1985).
6. N. J. Earhart, Ph.D. thesis, Lehigh University, 1989.
7. H. Warson, in *Emulsion Polymerization of Vinyl Acetate*, M. S. El-Aasser and J. W. Vanderhoff, Eds., Applied Science Publishers, New York, 1981, p. 1.
8. R. L. Zollars, in *Emulsion Polymerization of Vinyl Acetate*, M. S. El-Aasser and J. W. Vanderhoff, Eds., Applied Science Publishers, New York, 1981, p. 31.
9. A. S. Dunn and P. A. Taylor, *Makromol.*, **83**, 207–219 (1965).
10. A. Klein, C. H. Kuist, and V. T. Stannett, *J. Polym. Sci.*, **11**, 2111–2126 (1973).
11. D. C. Blackley, *Emulsion Polymerisation*, John Wiley & Sons, New York, 1975.
12. A. Netschey and A. E. Alexander, *J. Polym. Sci. A-1*, **8**: **1**, 399–405 (1970).
13. G. A. Johnson and K. E. Lewis, *Br. Polym. J.*, **1**, 266 (1969).
14. C.-S. Chern and G. W. Poehlein, *J. Appl. Polym. Sci.*, **33**, 2117–2136 (1987).
15. P. C. Hiemenz, *Principles of Colloid and Surface Chemistry*, Dekker, New York, 1977.

16. H. T. Kroener and V. L. Dimonie, in *Graduate Research Progress Reports, No. 34*, M. El-Aasser, E. S. Daniels, and E. D. Sudol, Eds., Emulsion Polymers Institute, Lehigh University, July 1990.
17. F. D. Hartley, *J. Polym. Sci.*, **34**, 397-417 (1959).
18. J. T. O'Donnell, R. B. Mesrobian, and A. E. Woodward, *J. Polym. Sci.*, **28**, 171-177 (1958).
19. S. Hayashi, K. Iwase, and N. Hojo, *Polym. J.*, **3**, 226-233 (1972).
20. D. Donescu, K. Gosa, I. Diaconescu, M. Mazare, and N. Carp, in *Emulsion Polymerization of Vinyl Acetate*, M. S. El-Aasser and J. W. Vanderhoff, Eds., Applied Science Publishers, New York, 1981, p. 203.
21. E. V. Gulbekian and G. E. J. Reynolds, in *Polyvinyl Alcohol: Properties & Applications*, C. A. Finch, Ed., John Wiley & Sons, New York, 1973, p. 427.
22. M. Nomura, M. Harada, W. Eguchi, and S. Nagata, in *Emulsion Polymerization: ACS Symp. Ser. No. 24*, I. Piirma and J. L. Gardon, Eds., ACS, Washington, D.C., 1976, p. 102.
23. Z. Song, Ph.D. thesis, Georgia Institute of Technology, 1988.
24. J. Ugelstad and F. K. Hansen, *Rubber Chem. and Tech.*, **49**, 536-609 (1976).

Received February 6, 1992

Accepted August 10, 1992